# STABILITY ANALYSIS OF TWO-STAGE HYDRAULIC CYLINDER

## M. Tech. Thesis


By

**Sumit Kumar Gupta**

**1802103024**



**DISCIPLINE OF MECHANICAL ENGINEERING**

**INDIAN INSTITUTE OF TECHNOLOGY INDORE**


**JUNE, 2020**

# STABILITY ANALYSIS OF TWO-STAGE HYDRAULIC CYLINDER

**A THESIS**

*Submitted in partial fulfillment of the requirements for the award of the degree*

***of***

**Master of Technology**

In

# Mechanical Engineering

*With specialization in*

# Mechanical System Design

*by*

**SUMIT KUMAR GUPTA**

**DISCIPLINE OF MECHANICAL ENGINEERING**

**INDIAN INSTITUTE OF TECHNOLOGY INDORE**

**JUNE, 2020**

# INDIAN INSTITUTE OF TECHNOLOGY INDORE

## CANDIDATE'S DECLARATION

I hereby certify that the work which is being presented in the thesis entitled **STABILITY ANALYSIS OF TWO-STAGE HYDRAULIC CYLINDER** in the partial fulfillment of the requirements for the award of the degree of **MASTER OF TECHNOLOGY** and submitted in the **DISCIPLINE OF MECHANICAL ENGINEERING, Indian Institute of Technology Indore**, is an authentic record of my own work carried out during the time period from July 2018 to June 2020 under the supervision of **Dr. Pavan Kumar Kankar, Associate Professor, Discipline of Mechanical engineering**.

The matter presented in this thesis has not been submitted by me for the award of any other degree of this or any other institute.

Sumit
14-06-2020

**Signature of the student with date**
**Sumit Kumar Gupta**

---

This is to certify that the above statement made by the candidate is correct to the best of my knowledge.

14/06/2020

**Dr. Pavan Kumar Kankar**

---

**Mr. Sumit Kumar Gupta** has successfully given his/her M.Tech. Oral Examination held on **23rd JUNE 2020**.

Signature(s) of Supervisor(s) of M. Tech. thesis
Date: 23-06-2020 (Dr. Pavan Kumar Kankar)

Convener, DPGC
Date: 29-06-2020

Signature of PSPC Member #1
Date: 23-06-2020 (Prof. Anand Parey)

Signature of PSPC Member #2
Date: 23-06-2020 (SI Kundalwal)

---

# ACKNOWLEDGEMENTS

My deepest appreciation is to my advisor, **Dr. Pavan Kumar Kankar**. I have been amazingly privileged to have an advisor who gave me the freedom to explore on my own and at the same time the guidance to recover when my steps faltered. His patience and support helped me to finish this dissertation.

I would like to thank my family and friends and the one above all of us, the omnipresent God for the support they provided.

A very special thanks to Mr. Jatin Prakash, Mr. Hirmukhe Sidram, Mr. Akash Sharma, Ms. Akanksha Chaudhari, Mr. Shivam Kumar, Mr. Eklavya Tripathi, Mr. Harshdeep Sharma & all my batch-mates for their moral support and supportive environment for completion of the work of IIT, Indore, India for their discussions throughout the project.

I will be failing in my duties if I do no extend my thanks to my mother Mrs. Chanda Gupta and my father Mr. Naresh Gupta, Brother Mr. Nawnit Gupta and Mr. Binit Gupta for their sincere advice and guidance. I would like to thank them all for their constant support and love.

Finally, I would like to thank the family of IIT Indore.

**DEDICATION**

***Dedicated***

***to***

***My beloved***

***Mom and Dad***

Abstract

A standard hydraulic cylinder consists of a piston rod with piston head and cylinder tube while a telescopic hydraulic cylinder consists of the two different cylinder tubes and a solid piston rod. It operates by the reciprocation of either piston rod or cylinder tube and mostly used to transmit mechanical power using the fluid linkage. The majority of the failures in hydraulic cylinders occur because of the buckling of the structure. Generally and more often, the piston rod is found to be failing in the buckling. This proposed work describes a new way of estimation of the buckling load of the telescopic hydraulic cylinder (two-stage) hinged at both extremes using Successive Approximation Method (SAM). SAM is traditionally applied to evaluate the buckling load in the bars where either the exact solution is not known or the mathematics is too complex. The method has been extended to the two-stage hydraulic cylinder with pin mounting boundary conditions at both the extremities. This method includes the number of iterations required to achieve better accuracy or in other words getting the minimum error. The critical load obtained after two iterations using the proposed method shows the minor deviation, i.e. it achieves the convergence.

Further, the projected method has been modified to incorporate the effect of misalignment between the cylinder tube and the piston rod at the piston head junction. The analytical procedure for the buckling load evaluation of telescopic hydraulic cylinder is described.

In continuation, finite element analysis of the hydraulic cylinder has also been performed to approximate and closely validate the findings using the analytical method of SAM. The Eigenvalue buckling analysis has been executed for the numerous dimensions of the hydraulic cylinder. Corresponding initial three buckling mode shape has also been described with the buckling load. The analytical buckling load and the simulated buckling load have been found in the close vicinity proving the approach

used in this study to be a good candidate for the buckling load estimation of the hydraulic cylinder.

# LIST OF PUBLICATION

- **Gupta S.K**., Prakash J., & Kankar, P. K. (2020). **Buckling load for telescopic cylinder using successive approximation method**. Indian Journal of Engineering and Materials Sciences, **(Accepted)**

# TABLE OF CONTENTS

# LIST OF FIGURES

# LIST OF TABLES

# NOMENCLATURE

| | | |
|---|---|---|
| $P$ | : | Axial force |
| $R$ | : | Concentrated load |
| $d$ | : | Distance between the station |
| $a$ & $b$ | : | Ordinates to the $\frac{M}{EI}$ |
| $c$ | : | Extrapolated values if for some reason, no actual value exists |
| $\frac{M}{EI}$ | : | Fictitious load |
| $P_{cr}$ | : | Critical load ($N$) |
| $E$ | : | Young's modulus of section $(N/mm^2)$ |
| $I$ | : | Moment of inertia of section ($mm^4$) |
| $L_{c1}$ | : | Length of 1st stage cylinder tube ($mm$) |
| $L_{c2}$ | : | Length of 2nd stage cylinder tube ($mm$) |
| $L_{s1}$ | : | Axial length between 2nd stage cylinder tube head and bearing ($mm$) |
| $L_{s2}$ | : | Axial length between piston head center and piston rod bearing ($mm$) |
| $L_p$ | : | length of the portion of piston rod exposed outside tube ($mm$) |
| $L_{ch}$ | : | Width of the cylinder head ($mm$) |

$L_{ph}$ : Width of the piston head ($mm$)

$D_{ce1}$ : Outer diameter of 1st stage cylinder tube ($mm$)

$D_{ci1}$ : Inner diameter of 1st stage cylinder tube ($mm$)

$D_{ce2}$ : Outer diameter of 2nd stage cylinder tube ($mm$)

$D_{ci2}$ : Inner diameter of 2nd stage cylinder tube ($mm$)

$\mathrm{d_p}$ : Diameter of the piston rod ($mm$)

$n$ : Number of stages of cylinder

$l$ : Total extended length

$Cl$ : Clearance

# ACRONYMS

| | |
|---|---|
| **FEA** | Finite Element Analysis |
| **SAM** | Successive Approximation Method |
| **CAE** | Computer-Aided Engineering |
| **FEM** | Finite Element Method |
| **CAD** | Computer-Aided Design |

# Chapter 1

# Introduction

## 1.1 Overview

The hydraulic cylinder is a mechanical actuation device which gets their power from pressurized hydraulic fluid and used to lift as well as to incline heavy loads under a controlled manner. A hydraulic cylinder majorly consisting of cylinder barrel and piston rod. It is widely used in dumpers, cranes and missile tilt to support the heavy load.

Figure 1.1 shows a systematic layout of the hydraulic cylinder. The excellence of the hydraulic cylinder is directly allied to the safety of the proposed machine. It also has some approximate impact on the reliability, loading and working efficiency and the maintenance cost. In this view, the design and improvement of a two-stage hydraulic cylinder are of utmost importance.

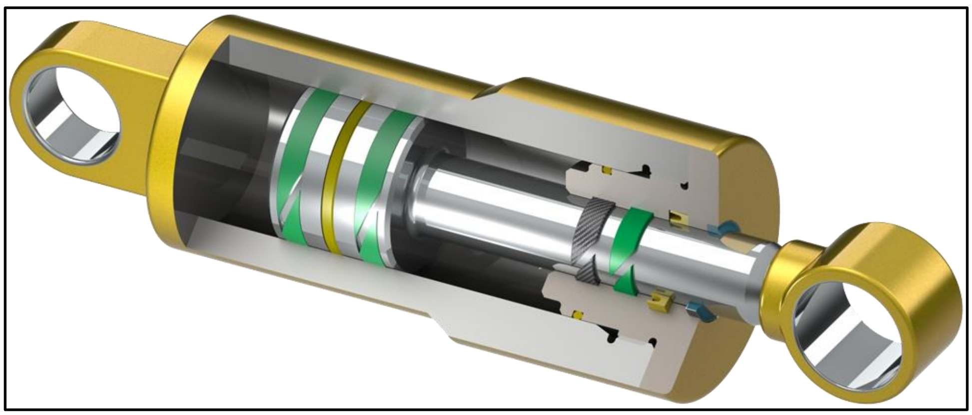

**Figure 1.1:** Section view of simple hydraulic cylinder [30].

As mentioned, normally a hydraulic cylinder (single-stage hydraulic cylinder) consists of a piston rod and a barrel, but in case of the telescopic hydraulic cylinder, it consists of a piston rod, a cylinder tube and several intermediate cylinders or rams. One of the main advantages of the telescopic cylinder over any other type of cylinders is that it provides exceptionally long output/stroke from a compact contracted length. Thus, when mounting space is limited and the application needs a long stroke a telescopic hydraulic cylinder is used.

Generally, the working environment is not even, sometimes everything goes smoothly whereas sometimes the condition gets worsened; thus, a hydraulic cylinder must be capable to perform better and efficiently. It should be enough stiff, strong and stable enough to support the load.

A hydraulic cylinder can be classified into the following categories according to their functional ability and specifications.

## 1.2 Classification of hydraulic cylinders

Based on the action of the piston rod in the cylinder tube, a hydraulic cylinder can be classified as:

- **i** **Single-acting cylinders:** Single acting cylinder is the most economical and simplest in design. In this type of hydraulic cylinder, the hydraulic fluid is pressurized from only one side of the cylinder during both the expansion as well as refutation process. It relies on the load, springs, other cylinders, or the momentum of a flywheel, to return the piston rod to its initial position when the fuel supply is cut-off. Because of its simpler design, there is less to maintain.
- **ii** **Double-acting cylinders:** In double-acting hydraulic cylinders, working fluid is provided interchangeably on both faces of the piston head. Double acting hydraulic cylinders are more common because of working applications at almost any angle. Single-acting cylinders cannot be used in large stroke applications because of inherent mechanical problems of springs.
- **iii** **Multi-stage/telescoping cylinder:** Multi-stage/telescopic cylinders can be either single or double-acting. They allow for a

long stroke while taking up much less space when collapsed. Due to the various segmentation, it increases the potential for piston flexion on piston design.

Based on the primary design styles of hydraulic cylinder construction used in industry, it can be broadly classified into the following categories.

i **Tie rod cylinder:** Tie-rod type hydraulic cylinders are most frequently employed in industrial applications due to its ability to get complete disassemble for the service and repair. Although this type of cylinder is not always customizable. It uses high strength threaded steel rods to hold the two end caps to the cylinder barrel.

ii **Welded body cylinder:** In this type of cylinder, the cylinder barrel is welded along with the end caps. Welded cylinders have a narrower body which enables them to fit better into the tight confines of machinery. Due to tie rod stretch, this type of cylinders does not suffer from failure at high pressures and long strokes.

## 1.3 Significance of the study

In industries, the hydraulic cylinders are designed according to Euler buckling theory assuming an equivalent column length. The Euler load estimation takes care of only structural failure, ignoring the material effort failure, which leads to a value for the critical load higher than the true value.

In the view of the above issues, a new methodology has been proposed and further modified in the present work to evaluate the realistic buckling load of the hydraulic cylinder. The scope and novelty of the present study can be described as:

- To study the Successive Approximation Method.
- To modify the Successive Approximation approach for the two-stage cylinder.

- To determine the buckling load of the two-stage cylinder.
- To study the clearance effect in the two-stage cylinder and to evaluate the buckling load (maximum load-carrying capacity).
- Implementation of the Finite Element Analysis (FEA) to obtain Eigenvalue buckling loads.

## 1.4 Organization of the thesis

A chapter-wise breakup of the present work is as follows:

**Chapter 1** provides an introduction and highlights the engineering applications of the hydraulic cylinder. Categorization of hydraulic cylinders has also been discussed based on the action of the piston in the cylinder tube and based on the primary design styles of hydraulic in industry. The objective of the present research work has been highlighted along with the organization of the thesis.

**Chapter 2** discusses a significant review of the published literature on the estimation of the buckling load. The section also mentions the findings of the Authors towards their contribution to the static and dynamic analysis for buckling.

**Chapter 3** describes the study of mathematical modelling based on Successive Approximation Method. This method has been adapted from single-stage to two-stage single-acting hydraulic cylinder with both ends pin-mounted for determining the buckling load of the critical buckling load. Further, the effect of clearance between inner annular of the cylinder tube and piston rod has also been studied. The effect of misalignment at the cylinder tube and piston head junction has also been considered to make the study more realistic.

**Chapter 4** describes the finite element approach for the estimation of the buckling load of the considered structure. The modelling of the hydraulic cylinder has also been described for a brief idea about FEA Modelling. The eigenvalues have been obtained for three initial mode shapes of buckling. Based on the mathematical modelling and Finite Element Method, the various result has been obtained using different quality of service parameters and graph analysing has also be done.

**Chapter 5** concludes and summarizes the research work and comprehensive discussions based on results obtained are presented. The scope of future work is also mentioned in this chapter.

# Chapter 2

# Review of Past Work

## 2.1 Introduction

This chapter conveys the detailed review of the buckling analysis of hydraulic cylinder as published by various authors in past. In a hydraulic cylinder, the estimation of the critical buckling load is of extreme importance. In this chapter, a summary of the different approaches adopted by researchers is provided. Various techniques, algorithms and different practices made by different academic and industry people have been discussed to meet more realistic approximations are listed.

## 2.2 History of hydraulic cylinder

The history of hydraulic is one of the innovative machinery components that make work easier and is a more efficient way to transfer mechanical power from one point to another. Most common uses of hydraulic cylinder in daily life can be found in cranes, tippers, compactors, drill rigs and dumpers and many more.

## 2.3 Critical load determination

Hoblit (1950) perhaps was the first to focus on evaluating the buckling load in the hydraulic cylinder. Hoblit considered it as a structural element. A typical fluid column was considered comprising an actuating cylinder, piston and piston rod. Hoblit concluded that the buckling load for a fluid column is the same as for a solid column having the same length and same moment of inertia [1]. Seshasai *et al.* (1975) discussed the various stresses in the hydraulic cylinders by considering the effect of initial imperfection with stroke. The combined effect of the axial load considering with effect of initial imperfection with stroke. Considering the variation in the crookedness angle with the increasing load in a vertically mounted both endpin supported hydraulic cylinder has been also examined. The effect of hydraulic pressure was also taken care of [2]. Ravishankar (1981) defined a method for the study of stresses and deflections in a hydraulic cylinder using a finite element analytical model. In this study, the author has divided the hydraulic cylinder into several finite elements generating stiffness matrices for each element and assembling the overall stiffness matrix. The crookedness angle and its components are calculated [3]. Barragetti *et al.* (1999) studied the effect of friction and the effect of clearance at the connection interface of the piston rod and the cylinder. Authors suggested an analytical method to determine the buckling behaviour for the hydraulic cylinder. Friction at the restrained ends, for both ends pin-mounted case, is also evaluated [5]. Barragetti *et al.* (2001) analyze the bending performance of double-acting hydraulic piston-type hydraulic actuators by means of analytical models considering rectilinear imperfections, friction and the actual geometric outline of piston-type actuators. The author also discussed the effects triggered by friction and clearance at the joining between the rod and the cylinder and also the friction at the restrained ends for pin ends [6]. ISO/Technical Standard 13725: 2001 considered the factor of safety standard explicated a method to estimate the cylinder buckling load for a single-stage hydraulic cylinder. The complete geometry of a fluid power cylinder is considered. Standard stated that since piston rod has less rigidity, it is more prone to buckle [7]. Codina and Salazar (2005) discussed an interpretation of the formulations for the calculation of the admissible load of buckling, to be applied in a fast and simple way in the field of the design, manufacture, selection and verification of hydraulic cylinders. Considering the critical parameters such as eccentricity, overload maximum allowable actuator has been studied to identify the effects of hydraulic cylinder for buckling load calculation [8]. Gamez-Montero *et al.* (2009) deliberated the effect of misalignment at the cylinder tube and piston rod interface. Authors mentioned that the interface is not perfectly rigid and misalignment occurs because of the flexibility of guide rings and clearance between components. There is no sudden buckling if there exist such types of initial imperfection. One important finding is that induced stresses and deflection increases gradually with increasing load and the effect of fluid compressibility reduces the imperfection angle between the piston rod and cylinder tube [10]. Gamez-Montero *et al.* (2009) deliberated an analytical approach based on the friction effects considering the effect of end supported friction on the loading capacity of the pin mounted hydraulic cylinder. The experimental study proposes that the actual critical buckling was nearer to the friction model compared to the frictionless end conditions [11]. Uzny (2009) discussed the effect of free vibration and stability of hydraulic cylinder using Euler force and elastically fixed at both ends. Based on Hamilton's principle for free vibration problem and minimum potential energy for the static problem the boundary value problem had been formulated. The natural frequency of the slender systems was also estimated considering the external load [12]. Shariati *et al.* (2010) studied the effects of length and boundary condition on the buckling and post-buckling behaviour of cylindrical panels. The buckling load decreases slightly with an increase in lengths. Also by increasing the sector angle of a panel, the buckling load increases [13]. Sui *et al*. (2010) discuss the design and analysis of a three-stage hydraulic cylinder used in dump trucks using CAE packages like Pro/E and ANSYS. The author concluded that this method is the significant way of improving the efficiency of design, shortening the design and trial-manufacture cycle of hydraulic cylinder and reducing the development cost. It also provides a convenient and practical analysis method for the design of the multistage hydraulic cylinder used in dump trucks [14]. Sui and Mio (2010) introduced the three-dimensional solid model of five-stage hydraulic cylinder design and analyzed, and the result shows that its bearing characteristics meet the requirements. The CAE technology used to design hydraulic cylinder can reduce costs, test and launching products times [15]. Flugge W (2013) introduced the effect of fluid pressure inside the cylinder on the buckling load and thus treated it as a fluid column [18].

Ramaswamy *et al*. (2017, 2018) discuss the buckling load calculation for the multistage hydraulic cylinder for both endpins mounted and fixed free condition. The author also studied the effect of internal clearance using the strain energy method. Further finite element analysis of multistage three-stage hydraulic cylinder has also been done for validation purpose. The author states that the effect of internal clearances which reduces the critical buckling load of hydraulic cylinders [25, 26]. Prakash *et al.* (2019, 2020) elaborated an analytical technique to calculate the maximum load-carrying capacity for the hydraulic cylinder with pin-mounted ends for single-stage and two-stage hydraulic cylinders. It also discusses the effect of stresses in the cylinder considering thin and thick cylinder theory. It concludes that the piston rod is more prone to buckle due to the less flexural rigidity [27, 28].

The purpose of this review was to view the trends and survey the current state of knowledge in the area of Eigenvalue buckling analysis of hydraulic cylinder. By identify theories and adding their ideas different theories and quantitative models have been generated and applied to estimate the buckling load. Most literature brush over the topic by fashioning their interpretation of concept models without truly understanding the nature of the many facets involved in the safety of designed products and structures. The number of research studies examining trust and its corresponding effect on industrial purpose success is relatively low. Thus, investigation of existing literature reveals a significant gap of research extends to the work of founding theorists of trust, empirical research, design and improvement.

In this presented thesis, Successive Approximation Method (SAM) [29] has been used iteratively for extraction of Eigenvalue buckling load. The proposed method includes a few numbers of iterations required in order to achieve good accuracy or in other words getting the minimum error. Further, finite element analysis of the hydraulic cylinder has also been performed for the validation purpose. The buckling mode shape for three different modes and their corresponding buckling load has also been obtained using the finite element method. The approximation of the buckling load corresponding to the first buckling mode shape has been performed and observed load lies in the close vicinity of theoretical calculation.

# Chapter 3

# Analytical Approach for the Determination of Buckling Load Using Successive Approximation Method

## 3.1 Introduction

Successive approximation method is a useful way to estimate the buckling load of a bar having different cross-section. The methods of successive approximations are used to determine critical loads in the case where the exact solution is unknown or very complicated where the energy methods always give a value for the critical load which is higher than the true value [29]. The methods of successive approximation provide a means of obtaining both lower and upper bound to the critical load. Thus the accuracy of the approximation solution is known and the successive approximation procedure can be continued until the desired accuracy is obtained.

Thus in the ongoing study, this method has been modified and adapted in order to estimate the buckling load of the two-stage single-acting hydraulic cylinder with both ends pin-mounted as follows:

- Buckling load determination without clearance.
- Buckling load determination considering clearance.

Figure 3.1 demonstrates the procedure adopted for the buckling load estimation using a Successive Approximation Method for two-stage hydraulic cylinder.

## 3.2 Buckling load determination considering no clearance

### 3.2.1 Overview

In section 3.2, a general technique for estimating Eigenvalue buckling load is modified and is presented for the mathematical improvement of an approximate eigenvalue Buckling load. There the technique is presented generally and, therefore, somewhat abstractly.

### 3.2.2 Methodology

The cylinder tube has been divided into 18 parts of equal length $\frac{l}{18}$. Because of the symmetry about Y-axis, the analysis can be done considering only half of the section as shown in Figure 3.2. The ratio of the second moment of the area of a piston rod and the cylinder barrel 1 $(I_1/I_3)$ is found to be 0.1142 whereas that of $(I_2/I_3)$ is 0.2867. Table 3.1 demonstrates the dimensions of the considered telescopic hydraulic cylinder. The deflection curve equation ( $y_1$ ) used for the first approximation for the buckled rod is given by the parabolic equation as

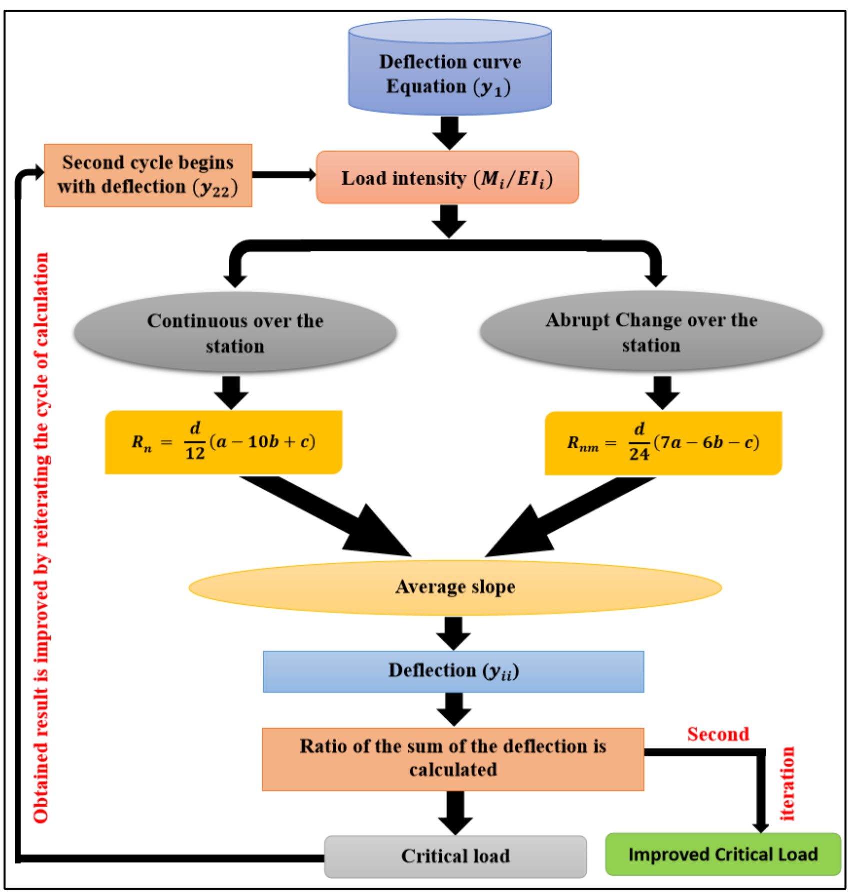


shown in equation 3.1.

**Figure 3.1:** Flow chart of procedure adapted for successive approximation method.

$$y_1 = \frac{4\delta x(l - x)}{l^2} \tag{3.1}$$

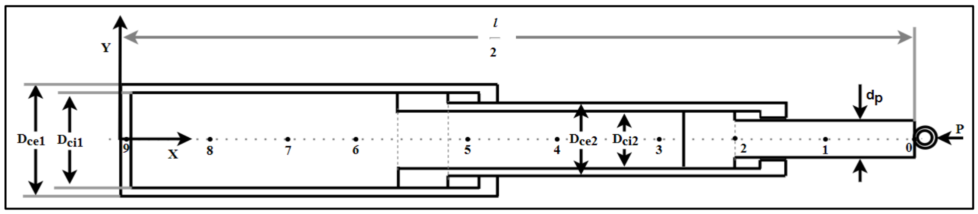


**Figure 3.2:** Half section view of the telescopic cylinder.

We know that the bending moment at any section of the bar is $M_i = Py_i$. In the next step, $M_1/EI_i$ is tabulated which represents the load intensity on the conjugate beam at the station points. These values are given by $Py_1/EI_i$. To calculate the concentrated load at different stations, two different methodologies have been adopted. The concentrated load $R_n$ is calculated, when the curve is continuous over the station points, as mentioned in equation 3.2 whereas, for junctions, when the load changes abruptly at the station points, the concentrated load is calculated using $R_{nm}$ as mentioned in equation 3.3.

$$R_n = \frac{d}{12}(a + 10b + c) \tag{3.2}$$

The values obtained using equation 3.2 and equation 3.3 are fed in their respective rows in Table 3.2. For example, the value of the concentrated load $R_1$ at station 1 is determined from equation 3.2 as shown below:

$$R_1 = \frac{d}{12}(a + 10b + c)$$

$$= \frac{l/18}{12}[(0 + 10(1.838) + 3.459)]\frac{\mathrm{P}\delta_1 l}{EI_3} = 0.1011\frac{\mathrm{P}\delta_1 l}{EI_3}$$

The same procedure can be successfully applied for the stations having continuous cross-section. For stations having an abrupt change in the $M/EI$ diagram, the fictitious reaction can be calculated as

$$R_{nm} = \frac{d}{24}(7a + 6b - c) \tag{3.3}$$

For example, the value of the concentrated load $R_2$ at station 2 is determined from equation 3.3 as shown below:

$$R_{21} = \frac{d}{24}(7a + 6b - c)$$

$$R_{21} = \frac{d}{24}\left[(7(3.459) + 6(1.838) - 0)\right]\frac{\mathrm{P}\delta_1 l}{EI_3} = 0.08158\,\frac{\mathrm{P}\delta_1 l}{EI_3}$$

$$R_{22} = \frac{d}{24}(7a + 6b - c)$$

$$R_{22} = \frac{d}{24}\left[(7(1.378) + 6(1.938) - 2.411)\right]\frac{\mathrm{P}\delta_1 l}{EI_3} = 0.04366\frac{\mathrm{P}\delta_1 l}{EI_3}$$

$$R_2 = R_{21} + R_{22} = 0.1252\frac{\mathrm{P}\delta_1 l}{EI_3}$$

The same procedure can be successfully applied for the stations having an abrupt change in the cross-section. This value is recorded in Table 3.2 as the fictitious shearing force or average slope. The fictitious reaction of the conjugate beam is

0.1011 + 0.1252 + 0.1073 + 0.1336 + 0.0975 + 0.04927 + 0.0527 + 0.05476 + $\frac{1}{2}$(0.05544) = 0.7491

Now, the average slope is determined using a simple average method considering the different number of the station parameters.

Next, the deflection ($y_{21}$) in the system is calculated directly from the average slope, noting that the deflection at station 1 is equal to the value of average slope in the first segments times the distance between the stations, whereas, the deflection at station 2 is equal to the deflection at 1 plus the next values of average slope times the distance between the station etc.

For example, the value of the deflection ($y_{21}$) at station 1 is determined from the average slope as shown below:

$$\frac{0.7163}{20} = 0.035815$$

Similarly, the value of the deflection ($y_{21}$) at station 2 is determined as

$$\frac{0.7163 + 0.6101}{20} = 0.06632$$

The same procedure can be successfully applied to obtain the value of the deflection ($y_{21}$) for different stations. Finally, the ratio of the new values of ($y_{21}$) are obtained by using the assumed value of $y_1$. Considering the minimum and maximum values of the ratios, it can be seen that the lower and upper limits for $P_{cr}$ are

$$5.86\frac{EI_3}{l^2} < P_{cr} < 9.506\frac{EI_3}{l^2}$$

The piston rod has been proved to be more prone to buckling failure because of its less flexural rigidity [1, 27]. Thus, from this point ahead, the buckling load for the system infers the buckling load for piston rod of the two-stage hydraulic cylinders.

As the length of each segment is constant for the given hydraulic cylinder, the ratio of $(y_1)_{av}$ to $(y_{21})_{av}$ is equal to the ratio of the sums of the deflection $y_1$ and $y_{21}$. Thus, the ratio of the sum of the deflection is shown in equation 3.4:

$$\frac{(y_1)_{av}}{(y_{22})_{av}} = \left(\frac{2\begin{pmatrix}0.2099 + 0.3951 + 0.5556 + 0.6914 + \\ 0.8025 + 0.8889 + 0.9506 + 0.987\end{pmatrix} + 1}{2\begin{pmatrix}0.03582 + 0.06632 + 0.07803 + 0.08862 + \\ 0.09633 + 0.09945 + 0.1026 + 0.1045\end{pmatrix} + 0.1052}\right)\left(\frac{EI_p}{Pl^2}\right)$$

$$P_{cr} = 8.258\ \frac{EI_p}{l^2} \tag{3.4}$$

$$P_{cr} = n * 8.258\ \frac{EI_p}{l^2} \tag{3.5}$$

Further, substituting the original dimensions and the material properties in equation 3.5, $P_{cr}$ is determined as follows in Table 3.1.

The obtained result is improved by reiterating the cycle of calculation as shown in Table 3.2. The second cycle begins with deflection $y_{22}$ which are proportional to the deflection $y_{21}$ found from the first set of computations.

$$y_{22} = \frac{16\delta_2 x}{5l}\left(1 - \frac{2x^2}{l^2} + \frac{x^3}{l^3}\right) \tag{3.6}$$

where $\delta_2$ equals the deflection at the centre of the hydraulic cylinder. In the next step, $M_2/EI_i$ are tabulated and represent the intensities of load on conjugate beam at the station points. These values are equal to $Py_{22}/EI_i$ .

The result of the second cycle shows that the load $P_{cr}$ lies between

$$5.859\frac{EI_p}{l^2} < P_{cr} < 9.97\frac{EI_p}{l^2}$$

The values obtained by taking the ratio of the sums of the deflection is

$$\frac{(y_{22})_{av}}{(y_{33})_{av}} = \left(\frac{\left(2\begin{pmatrix}0.1767 + 0.3473 + 0.506 + 0.6487 + \\ 0.7708 + 0.8691 + 0.9412 + 0.9852\end{pmatrix}\right) + 1}{\left(2\begin{pmatrix}0.03016 + 0.0583 + 0.07002 + 0.08116 + 0.08977 \\ +0.09355 + 0.09726 + 0.09952\end{pmatrix}\right) + 0.1003}\right)\left(\frac{EI_p}{Pl^2}\right)$$

$$P_{cr} = 8.576\frac{EI_p}{l^2} \tag{3.7}$$

Since the value is seen in Table 3.2, $P_{cr} = 9.97$ and thus it is seen that nearly accurate results have been obtained in the two-cycle of successive approximation computations. The numerical example is as shown below:

$$P_{cr} = n * 8.576\frac{EI_p}{l^2} \tag{3.8}$$

where

E = 220000 $\frac{N}{mm^2}$ , $I_p = \frac{\pi}{64}\, d^4$ , $d_p$ = 24 mm & n = 2

**Table 3.1:** Buckling load determination.

| **Dimensions of the telescopic hydraulic cylinder (mm)** | | | | | | | | | **Buckling load on the First iteration (N)** | **Buckling load on the Second iteration (N)** |
|---|---|---|---|---|---|---|---|---|---|---|
| $l$ | $L_{c_1}$ | $L_{c_2}$ | $L_p$ | $D_{ce_1}$ | $D_{ci_1}$ | $D_{ce_2}$ | $D_{ci_2}$ | $d_p$ | | |
| **1501.5** | 535 | 495 | 485 | 72 | 60 | 60 | 48 | 24 | 26247.72 | 27258.48 |
| **1441.5** | 515 | 475 | 465 | 72 | 60 | 60 | 48 | 24 | 28478.238 | 29574.8821 |
| **991.5** | 365 | 325 | 315 | 72 | 60 | 60 | 48 | 24 | 60194.52 | 62512.50 |
| **751.5** | 285 | 245 | 235 | 72 | 60 | 60 | 48 | 24 | 104781.46 | 108816.398 |

**Table 3.2** Successive approximation method results considering no clearance.

<table>
<tr><th>Station number</th><th>0</th><th colspan="2">1</th><th colspan="2">2</th><th colspan="2">3</th><th colspan="2">4</th><th colspan="2">5</th><th colspan="2">6</th><th colspan="2">7</th><th colspan="2">8</th><th>9</th><th>Common Factor</th></tr>
<tr><td>$y_1$</td><td>0</td><td colspan="2">0.2099</td><td colspan="2">0.3951</td><td colspan="2">0.5556</td><td colspan="2">0.6914</td><td colspan="2">0.8025</td><td colspan="2">0.8889</td><td colspan="2">0.9506</td><td colspan="2">0.9877</td><td>1</td><td>$\delta_1$</td></tr>
<tr><td>$M_1/EI$</td><td>0</td><td colspan="2">1.838</td><td>3.459</td><td>1.378</td><td colspan="2">1.938</td><td colspan="2">2.411</td><td>2.799</td><td>0.8025</td><td colspan="2">0.8889</td><td colspan="2">0.9506</td><td colspan="2">0.9877</td><td>1</td><td>$\frac{P\delta_1}{EI_3}$</td></tr>
<tr><td>R</td><td></td><td colspan="2">0.1011</td><td colspan="2">0.1252</td><td colspan="2">0.1073</td><td colspan="2">0.1336</td><td colspan="2">0.0975</td><td colspan="2">0.04927</td><td colspan="2">0.0527</td><td colspan="2">0.05476</td><td>0.05544</td><td>$\frac{P\delta_1 l}{EI_3}$</td></tr>
<tr><td>Average slope</td><td colspan="2">0.7163</td><td colspan="2">0.6101</td><td colspan="2">0.2342</td><td colspan="2">0.2117</td><td colspan="2">0.1543</td><td colspan="2">0.06228</td><td colspan="2">0.06342</td><td colspan="2">0.03778</td><td colspan="2">0.01299</td><td>$\frac{P\delta_1 l}{EI_3}$</td></tr>
<tr><td>$y_{21}$</td><td>0</td><td colspan="2">0.03582</td><td colspan="2">0.06632</td><td colspan="2">0.07803</td><td colspan="2">0.08862</td><td colspan="2">0.09633</td><td colspan="2">0.09945</td><td colspan="2">0.1026</td><td colspan="2">0.1045</td><td>0.1052</td><td>$\frac{P\delta_1 l^2}{EI_3}$</td></tr>
<tr><td>$y_1/y_{21}$</td><td></td><td colspan="2">5.86</td><td colspan="2">5.957</td><td colspan="2">7.12</td><td colspan="2">7.802</td><td colspan="2">8.311</td><td colspan="2">8.9738</td><td colspan="2">9.265</td><td colspan="2">9.445</td><td>9.506</td><td>$\frac{EI_3}{Pl^2}$</td></tr>
<tr><td colspan="20"></td></tr>
<tr><td>$y_{22}$</td><td>0</td><td colspan="2">0.1767</td><td colspan="2">0.3473</td><td colspan="2">0.506</td><td colspan="2">0.6487</td><td colspan="2">0.7708</td><td colspan="2">0.8691</td><td colspan="2">0.9412</td><td colspan="2">0.9852</td><td>1</td><td>$\delta_2$</td></tr>
<tr><td>$M_2/EI$</td><td>0</td><td colspan="2">1.547</td><td>3.041</td><td>1.214</td><td colspan="2">1.77</td><td colspan="2">2.268</td><td>2.695</td><td>0.7708</td><td colspan="2">0.8691</td><td colspan="2">0.9412</td><td colspan="2">0.9852</td><td>1</td><td>$\frac{P\delta_2}{EI_3}$</td></tr>
<tr><td>R</td><td></td><td colspan="2">0.0857</td><td colspan="2">0.1098</td><td colspan="2">0.09806</td><td colspan="2">0.1257</td><td colspan="2">0.09344</td><td colspan="2">0.04816</td><td colspan="2">0.05216</td><td colspan="2">0.0546</td><td>0.05542</td><td>$\frac{P\delta_2 l}{EI_3}$</td></tr>
<tr><td>Average slope</td><td colspan="2">0.6031</td><td colspan="2">0.5629</td><td colspan="2">0.2343</td><td colspan="2">0.2228</td><td colspan="2">0.1723</td><td colspan="2">0.07566</td><td colspan="2">0.0741</td><td colspan="2">0.04522</td><td colspan="2">0.01521</td><td>$\frac{P\delta_2 l}{EI_3}$</td></tr>
<tr><td>$y_{33}$</td><td></td><td colspan="2">0.03016</td><td colspan="2">0.0583</td><td colspan="2">0.07002</td><td colspan="2">0.08116</td><td colspan="2">0.08977</td><td colspan="2">0.09355</td><td colspan="2">0.09726</td><td colspan="2">0.09952</td><td>0.1003</td><td>$\frac{P\delta_2 l^2}{EI_3}$</td></tr>
<tr><td>$y_{22}/y_{33}$</td><td></td><td colspan="2">5.859</td><td colspan="2">5.957</td><td colspan="2">7.227</td><td colspan="2">7.993</td><td colspan="2">8.586</td><td colspan="2">9.29</td><td colspan="2">9.677</td><td colspan="2">9.9</td><td>9.97</td><td>$\frac{EI_3}{Pl^2}$</td></tr>
</table>

## 3.3 Buckling load determination considering clearance

### 3.3.1 Overview

In section 3.3, the solution process for the buckling of a hydraulic cylinder is presented in mathematical modelling considering clearance at the tip of the cylinder and piston rod. The methodology obtained is the same as section 3.2.

### 3.3.2 Methodology

The method has been thus modified to study the misalignment effect on estimating the buckling load when the piston is misaligned and modified to estimate the maximum load-carrying capacity of the two-stage hydraulic cylinder with both ends pin-mounted.

To estimate the critical load of a bar having dissimilar cross-section Successive approximation method is a useful way. Thus, in the fragmentary study, this method has been improved and modified to estimate the buckling load of the two-stage single-acting hydraulic cylinder considering clearance at the cylinder 2 and piston rod with both

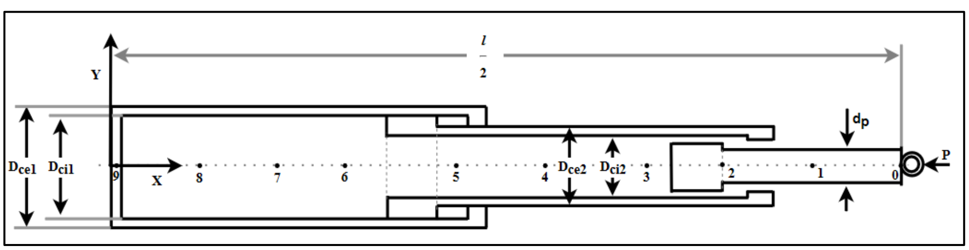


ends hinged.

**Figure 3.3**: Half section view of the telescopic cylinder considering clearance.

The cylinder tube has been alienated into 18 parts of equal length $\frac{l}{18}$. For the reason that of the symmetry about Y-axis, the analysis can be done bearing in mind only half of the section as presented in Figure 3.3. The ratio of the second moment of the area of a piston rod and the cylinder barrel 1 $(I_1/I_3)$ is found to be 0.1142 whereas that of $(I_2/I_3)$ is 0.2867.

The deflection curve equation considering clearance effect $(y_1)$ used for the first approximation for the buckled rod is given by the parabolic equation as shown in equation 3.9.

$$y_{11} = \delta_1 \left[ \frac{4x(l-x)}{l^2} + \frac{\sin\left(\frac{\pi}{L_{c2}/L_p + 1}\right)}{\sin\left(\frac{\pi x}{l}\right)} \right] \tag{3.9}$$

We know that the bending moment at any section of the bar is $M_i = Py_i$.

In the next step, $M_1/EI_i$ is charted which signifies the load intensity on the conjugate beam at the station points. These values are given by $Py_1/EI_i$.

To compute the concentrated load at dissimilar stations two different practises having been adopted. The concentrated load $R_n$ is used when the curve is continuous over the station points, as mentioned in equation 3.10 whereas, for junctions, when the load changes brusquely at the station points, the concentrated load is calculated using $R_{nm}$ as mentioned in equation 3.11.

$$R_n = \frac{d}{12}(a + 10b + c) \tag{3.10}$$

The values obtained using equation 3.10 and equation 3.11 are fed into the in their respective rows.

The same technique can be effectively applied for the stations having continuous cross-section. For stations having an abrupt change in the $M/EI$ diagram, the fictitious reaction can be calculated as

$$R_{nm} = \frac{d}{24}(7a + 6b - c) \tag{3.11}$$

The same technique can be successfully applied for the stations having an abrupt change in the cross-section as shown in equation 3.10 and 3.11. This value is noted in Table 3.4 as the fictitious shearing force or average slope. The fictitious reaction of the conjugate beam is

0.242 + 0.3045 + 0.2662 + 0.3366 + 0.2483 + 0.127 + 0.1368 + 0.1427 + $\frac{1}{2}$(0.1447) = 0.7491

Now, the average slope is estimated using a simple average method considering the different number of the station parameters. Next, the deflection ($y_{21}$) in the system is calculated directly from the average slope, noting that the deflection at station 1 is equal to the value of average slope in the first segments times the distance between the stations, whereas, the deflection at station 2 is equal to the deflection at 1 plus the next values of average slope times the distance between the station etc.

The same procedure can be successfully applied to obtain the value of the deflection ($y_{21}$) for different stations. Finally, the ratio of the new values of $y_{21}$ are obtained by using the assumed value of $y_1$. Considering the minimum and maximum values of the ratios, it can be seen that the lower and upper limits for $P_{cr}$ are

$$5.859\frac{EI_3}{l^2} < P_{cr} < 9.765\frac{EI_3}{l^2}$$

As the length of each segment is constant for the given hydraulic cylinder, the ratio of $(y_1)_{av}$ to $(y_{21})_{av}$ is equal to the ratio of the sums of the deflection $y_1$ and $y_{21}$. Thus, for the ratio of the sum of the deflection:

$$\frac{(y_1)_{av}}{(y_{22})_{av}} = \frac{2\begin{pmatrix}0.5007 + 0.9623 + 1.378 + 1.742 + \\ 2.048 + 2.291 + 2.468 + 2.575\end{pmatrix} + 2.611}{2\begin{pmatrix}0.08545 + 0.1615 + 0.192 + 0.2204 + \\ 0.2418 + 0.2509 + 0.26 + 0.2655\end{pmatrix} + 0.2674}\ \frac{EI_p}{Pl^2}$$

$$P_{cr} = 8.430\ \frac{EI_p}{l^2} \tag{3.12}$$

$$P_{cr} = n * 8.430\ \frac{EI_p}{l^2} \tag{3.13}$$

Substituting the original dimensions from Table 3.3 and the material properties in equation 3.13, $P_{cr}$ is determined as follows:

The obtained result is improved by reiterating the cycle of calculation as shown in Table 3.4. The second cycle begins with deflection $y_{22}$ which are proportional to the deflection $y_{21}$ found from the first set of computations.

$$y_{22} = \delta_2 \left[ \left\{ \frac{16x}{5l} \left( 1 - \frac{2x^2}{l^2} + \frac{x^3}{l^3} + \right) \right\} + \frac{\sin\left(\frac{\pi}{L_{c2}/L_p + 1}\right)}{\sin\left(\frac{\pi x}{l}\right)} \right] \tag{3.14}$$

where $\delta_2$ equals the deflection at the centre of the hydraulic cylinder. In the next step, $M_2/EI_i$ are tabulated and represent the intensities of load on conjugate beam at the station points. These values are equal to $Py_{22}/EI_i$ . The result of the second cycle shows that the load $P_{cr}$ lies between

$$5.858 \frac{EI_p}{l^2} < \ P_{cr} < \ 9.97 \frac{EI_p}{l^2}$$

The values obtained by taking the ratio of the sums of the deflection is

$$\frac{(y_{22})_{av}}{(y_{33})_{av}} = \left( \frac{2\begin{pmatrix} 0.4574\ +\ 0.8999\ +\ 1.314\ +\ 1.686\ +\ 2.006 \\ +\ 2.265\ +\ 2.456\ +\ 2.572 \end{pmatrix} + 2.611}{2\begin{pmatrix} 0.07807\ +\ 0.1511\ +\ 0.1815\ +\ 0.2106 \\ +\ 0.2331\ +\ 0.2431\ +\ 0.2529\ +\ 0.2589 \end{pmatrix} + 0.2609} \right)$$

$$\left( \frac{EI_p}{Pl^2} \right)$$

$$P_{cr} = 8.599 \frac{EI_p}{l^2} \tag{3.15}$$

$$P_{cr} = n * 8.599 \frac{EI_p}{l^2} \tag{3.16}$$

Since the value is seen in Table 3.4, $P_{cr} = 9.97$ and thus it is seen that nearly accurate results have been obtained in the two-cycle of successive approximation computations. Substituting the original dimensions and the material properties in equation 3.16, $P_{cr}$ is determined as follows as shown below in Table 3.3.

where,

E = 220000 $\frac{N}{mm^2}$ , $I_p = \frac{\pi}{64} d^4$ , $l$ = 1441.5 mm & n = 2

**Table 3.3:** Buckling load determination considering clearance.

| **Clearance (cl)** | **Dimensions of telescopic hydraulic cylinder (mm)** | | | | | | | | | **Buckling load on First iteration(N)** | **Buckling load on Second iteration (N)** |
|---|---|---|---|---|---|---|---|---|---|---|---|
| | $l$ | $L_{c_1}$ | $L_{c_2}$ | $L_p$ | $D_{ce_1}$ | $D_{ci_1}$ | $D_{ce_2}$ | $D_{ci_2}$ | $d_p$ | | |
| **0.325** | 1441.5 | 515 | 475 | 465 | 72 | 60 | 60 | 48 | 23.675 | 2.7528e+04 | 28080.26 |
| **0.5** | 1441.5 | 515 | 475 | 465 | 72 | 60 | 60 | 48 | 23.5 | 2.6723e+04 | 27259.17 |
| **0.85** | 1441.5 | 515 | 475 | 465 | 72 | 60 | 60 | 48 | 23.15 | 2.5167e+04 | 25671.14 |

**Table 3.4:** Successive approximation method results considering clearance.

| Station number | 0 | 1 | 2 | | 3 | 4 | 5 | | 6 | 7 | 8 | 9 | Common Factor |
|---|---|---|---|---|---|---|---|---|---|---|---|---|---|
| $y_1$ | 0 | 0.5007 | 0.9623 | | 1.378 | 1.742 | 2.048 | | 2.291 | 2.468 | 2.575 | 2.611 | $\delta_1$ |
| $M_1/EI$ | 0 | 4.384 | 8.426 | 3.356 | 4.806 | 6.075 | 7.142 | 2.048 | 2.291 | 2.468 | 2.575 | 2.611 | $\frac{P\delta_1}{EI_3}$ |
| R | | 0.242 | 0.3045 | | 0.2662 | 0.3366 | 0.2483 | | 0.127 | 0.1368 | 0.1427 | 0.1447 | $\frac{P\delta_1 l}{EI_3}$ |
| Average slope | | 1.709 | 1.522 | | 0.6092 | 0.5676 | 0.4283 | | 0.1827 | 0.1817 | 0.1102 | 0.03695 | $\frac{P\delta_1 l}{EI_3}$ |
| $y_{21}$ | 0 | 0.08545 | 0.1615 | | 0.192 | 0.2204 | 0.2418 | | 0.2509 | 0.26 | 0.2655 | 0.2674 | $\frac{P\delta_1 l^2}{EI_3}$ |
| $y_1/y_{21}$ | | 5.859 | 5.957 | | 7.177 | 7.903 | 8.469 | | 9.13 | 9.491 | 9.698 | 9.765 | $\frac{EI_3}{Pl^2}$ |
| | | | | | | | | | | | | | |
| $y_{22}$ | 0 | 0.4574 | 0.8999 | | 1.314 | 1.686 | 2.006 | | 2.265 | 2.456 | 2.572 | 2.611 | $\delta_2$ |
| $M_2/EI$ | 0 | 4.005 | 7.88 | 3.139 | 4.582 | 5.881 | 6.998 | 2.006 | 2.265 | 2.456 | 2.572 | 2.611 | $\frac{P\delta_2}{EI_3}$ |
| R | | 0.2219 | 0.2842 | | 0.2539 | 0.3259 | 0.2428 | | 0.1255 | 0.1361 | 0.1425 | 0.1447 | $\frac{P\delta_2 l}{EI_3}$ |
| Average slope | | 1.561 | 1.46 | | 0.6088 | 0.5812 | 0.4515 | | 0.2003 | 0.1956 | 0.1195 | 0.04022 | $\frac{P\delta_2 l}{EI_3}$ |
| $y_{33}$ | | 0.07807 | 0.1511 | | 0.1815 | 0.2106 | 0.2331 | | 0.2431 | 0.2529 | 0.2589 | 0.2609 | $\frac{P\delta_2 l^2}{EI_3}$ |
| $y_{22}/y_{33}$ | | 5.858 | 5.957 | | 7.237 | 8.007 | 8.606 | | 9.316 | 9.708 | 9.934 | 9.97 | $\frac{EI_3}{Pl^2}$ |

# Chapter 4

# Estimation of Eigenvalue Buckling Load Using Finite Element Analysis

## 4.1 Introduction

Engineers are exclusively responsible for the reliability and safety of designed products and structures. Minor errors in design often lead to looming ruins. This is why they endure an array of testing and optimization before being arrayed in everyday life. But doing so over many iterations will be excessively expensive. So design engineers often look to simulation modelling practices (like Finite Element Analysis using Computer-Aided Engineering packages) to systematize and make things easier while testing. This helps to cut back the employment of materials for iterative prototyping, which might rather be utilized in actualization.

Thus, the finite element method (FEM) has been proved a powerful approach, to reach a realistic solution which also reduced time, error efforts and cost. Even though it does not offer precise results, it achieves the nearby results.

Some of the advantages of using FEA are:

- Simulation of a designed model can be created instead of having a physical model for testing purposes.
- FEM analysis allows choosing a various number of material types.
- FEA also have the ability to observe impact effects on a minor area of design in complex geometry.

## 4.2 Buckling load validation considering no clearance

### 4.2.1 Overview

In this section, a general technique for estimating Eigenvalue buckling load is modified and is presented for the mathematical improvement of an approximate eigenvalue Buckling load.

### 4.2.2 Methodology

The specified pinned mounting hydraulic cylinder has been analysed by linear elastic static finite element analysis as presented in Figure 4.1 using Abaqus. In the considered simulation, the linear elastic isotropic element has been considered with the properties as mentioned in Table 4.1.

**Table 4.1:** Properties used in simulation.

| **Property Name** | **Property value/ Characteristic** |
|---|---|
| Section type | Solid homogeneous |
| Young's Modulus | 220000 $N/mm^2$ |
| Poisson's ratio | 0.27 |
| Mass density | $7.8*10^{-6}$ |

For the simulation purpose, the cylinder has been treated similar to a pinned beam at both extremes. The boundary conditions have been provided at both the ends. At the piston rod end, two degrees of freedom i.e. longitudinal displacement (x-axis) and the rotation about a perpendicular axis (z-axis) is allowed. At another hinged end, displacement along all three axes have been seized and only rotation about the perpendicular axis (z-axis) is allowed to take place. To realise the buckling load of the cylinder, an open centred length of the structure has been used. In other words, fully extracted cylinder has been kept under investigation. Further, *c3d8r*, linear brick elements of element size 25 has been found suitable to carry out the simulation. The modelled hydraulic cylinder is shown in Figure 4.2. The compressive load, concentrated in nature has been applied at piston rod end and is increased stepwise from 1 N till the buckling is noticed. Figure 4.3 (a)-(c) shows the simulation results of the buckling performed in Abaqus for 535 mm, 495 mm long cylinder tube in 1st and 2nd stage respectively with piston rod of length 485 mm. Figure 4.4 (a)-(c) resembles the same results for different dimension of the articulation in the structure. It shows the results while considering 515 mm, 475 mm long cylinder tube in 1st and 2nd stage respectively with piston rod of length 465 mm.

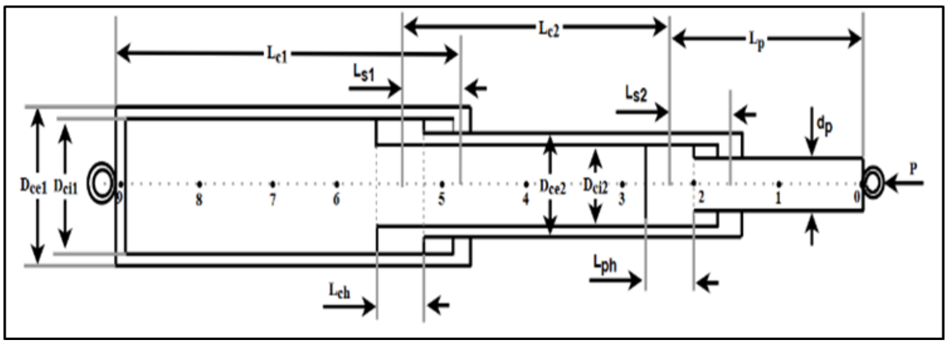


**Figure 4.1:** Diagrammatic representation of half of the hydraulic cylinder used in numerical simulation.

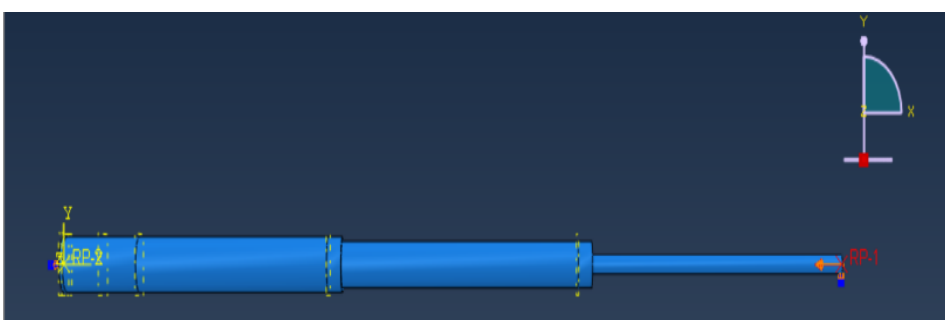

**Figure 4.2:** CAD model of the telescopic cylinder.

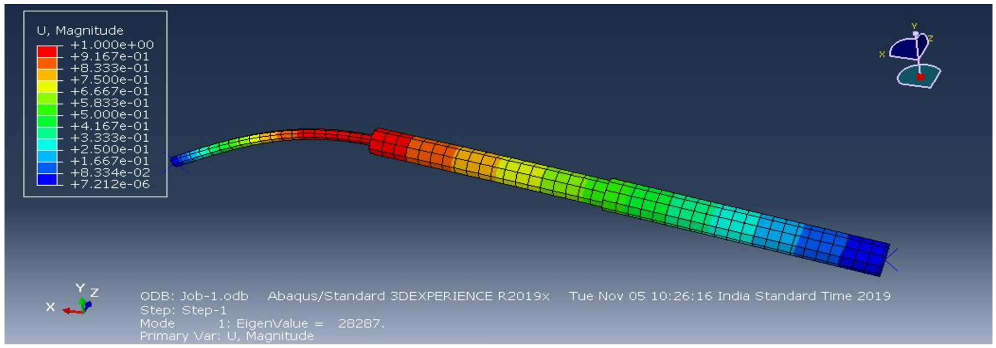


(a.)

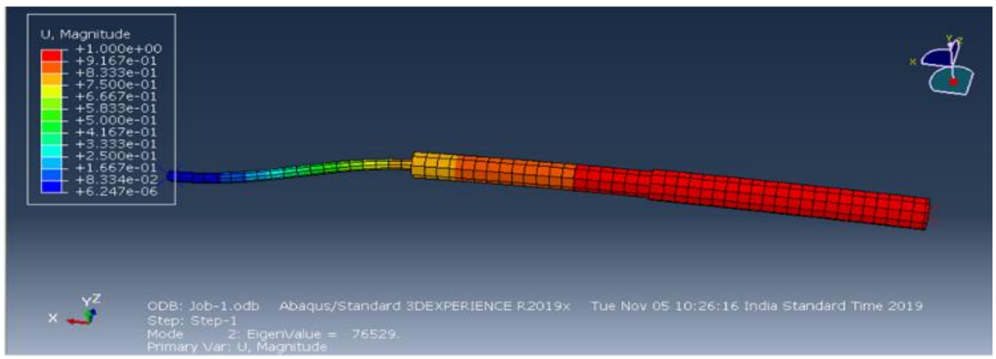


(b.)

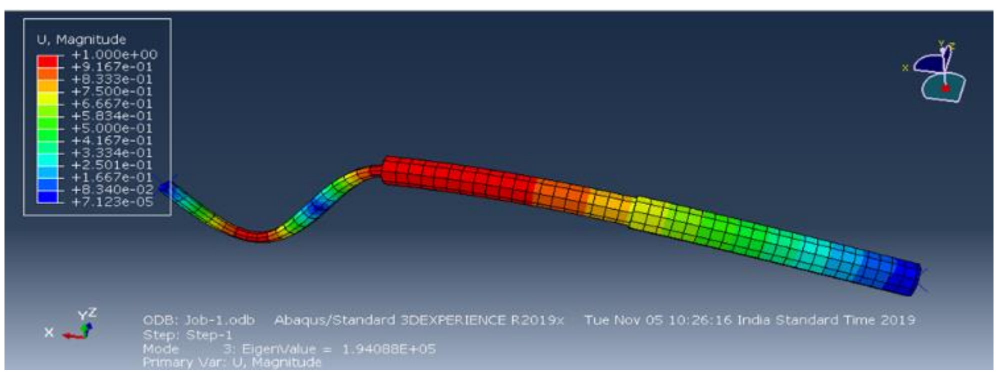


(c.)

**Figure 4.3:** (a)-(c) Eigenvalue buckling load for 535 mm, 495 mm long cylinder tube in 1$^{st}$ and 2$^{nd}$ stage respectively with piston rod of length 485 mm with mode shape 1$^{st}$, 2$^{nd}$ and 3$^{rd}$.

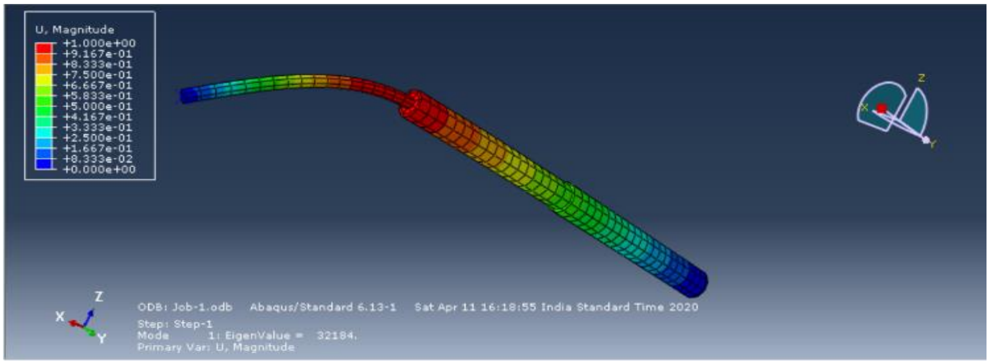


(a.)

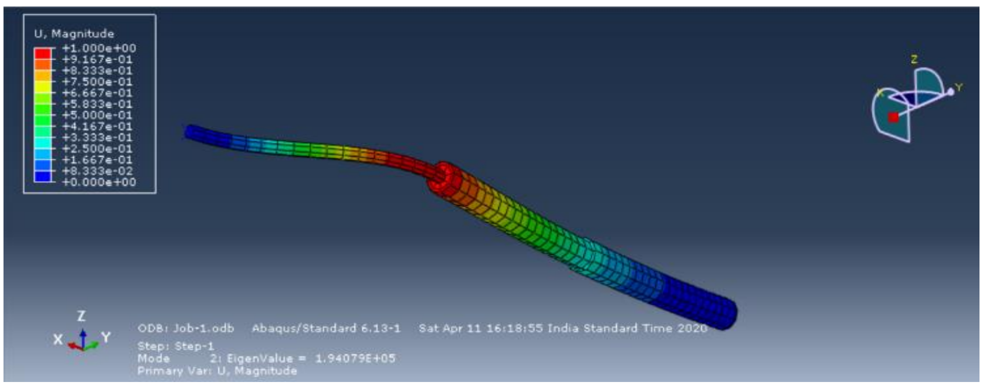


(b.)

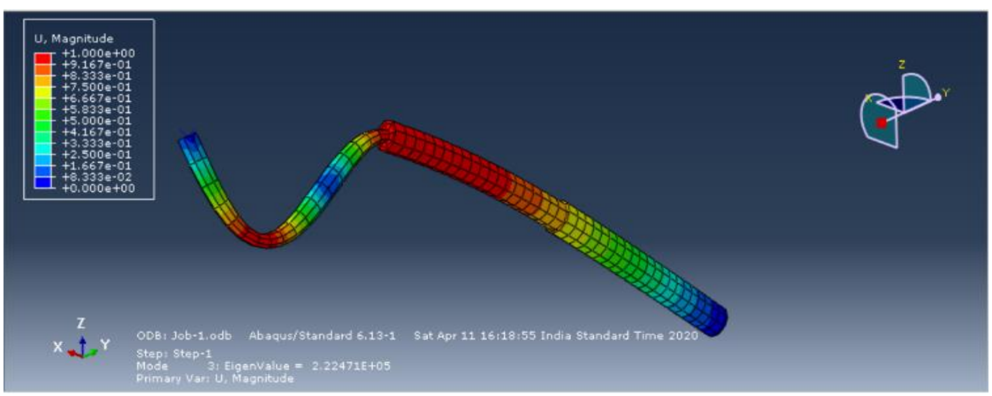


(c.)

**Figure 4.4:** (a)-(c) Eigenvalue buckling load for 515 mm, 475 mm long cylinder tube in 1$^{st}$ and 2$^{nd}$ stage respectively with piston rod of length 465 mm with mode shape 1$^{st}$, 2$^{nd}$ and 3$^{rd}$.

## 4.3 Buckling load validation considering clearance

### 4.3.1 Overview

In this section, the solution process for the buckling of a hydraulic cylinder is presented in mathematical modelling considering clearance at the tip of the cylinder tube and the piston rod.

The method has been thus modified to examine the misalignment effect on estimating the buckling load when the piston is misaligned and adapted to calculate the maximum load-carrying capacity of the two-stage hydraulic cylinder with both ends pin-mounted.

### 4.3.2 Methodology

The specified pinned mounting hydraulic cylinder has been analysed by linear elastic static finite element analysis as presented in Figure. 4.5. Figure 4.6 shows the zoomed view of the highlighted region. The material properties have been considered the same as mentioned in Table 4.1. The boundary conditions have also been applied as stated in section 4.2.2. The similar approach mentioned in the section 4.2.2 has been incorporated to observe the buckling of the structure considering the misalignment at the connection head of 2$^{nd}$ stage cylinder tube and the piston rod. Element type and the size used in the simulation have also been kept identical to that of the former.

Figure. 4.7 displays the results as well as the shape of the structure after buckling with 515 mm, 475 mm long cylinder tube in 1$^{st}$ and 2$^{nd}$ stage respectively and piston rod of length 465 mm considering a clearance of 0.325 mm at the tip of 2$^{nd}$ stage cylinder tube and piston rod for initial three buckling modes. Their respective buckling load in accordance with Eigenvalue buckling is also mentioned in the relevant figures. Likewise, Figure 4.8 and Figure 4.9 contain the results carried out for similar simulations, considering a clearance of 0.50 mm and 0.85 mm respectively at the tip of 2$^{nd}$ stage cylinder tube and piston rod.

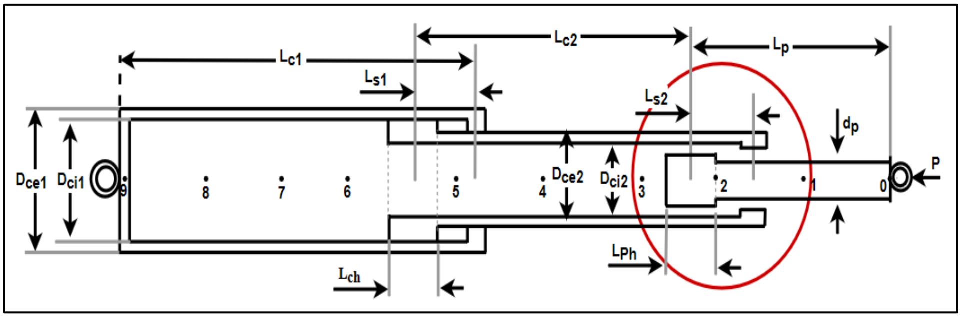


**Figure 4.5:** Half section view of the telescopic cylinder considering clearance at the tip of 2nd stage cylinder tube and piston rod.

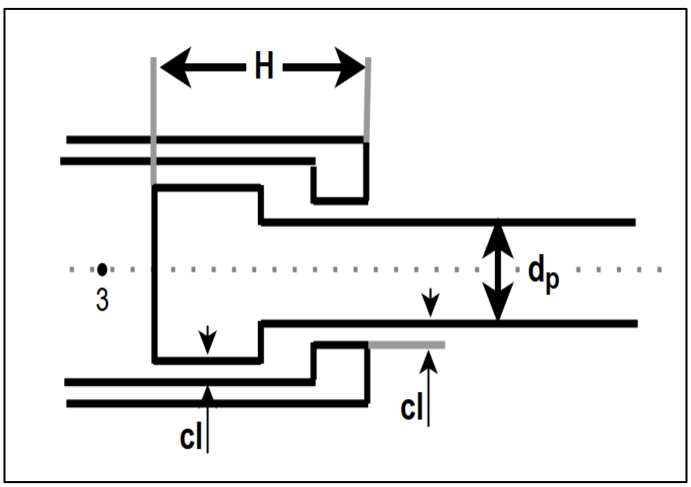


**Figure 4.6**: Zoomed view of highlighted region.

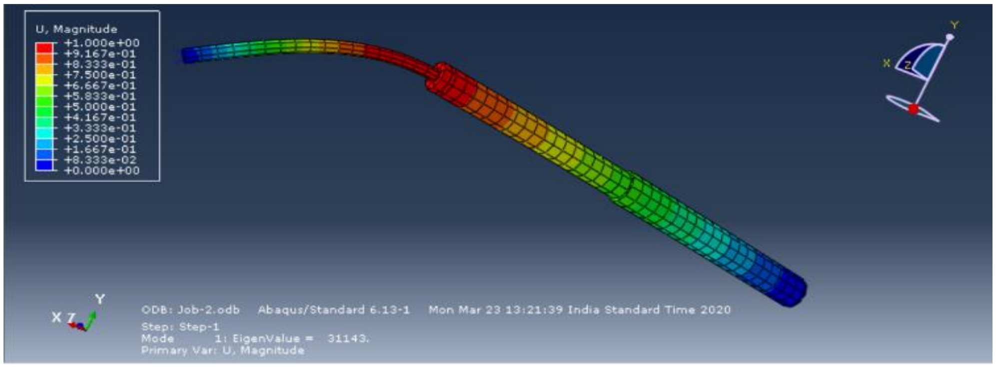


(a.)

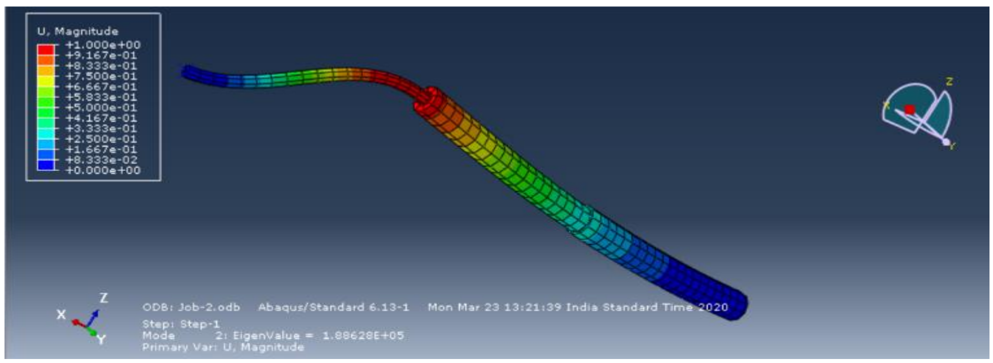


(b.)

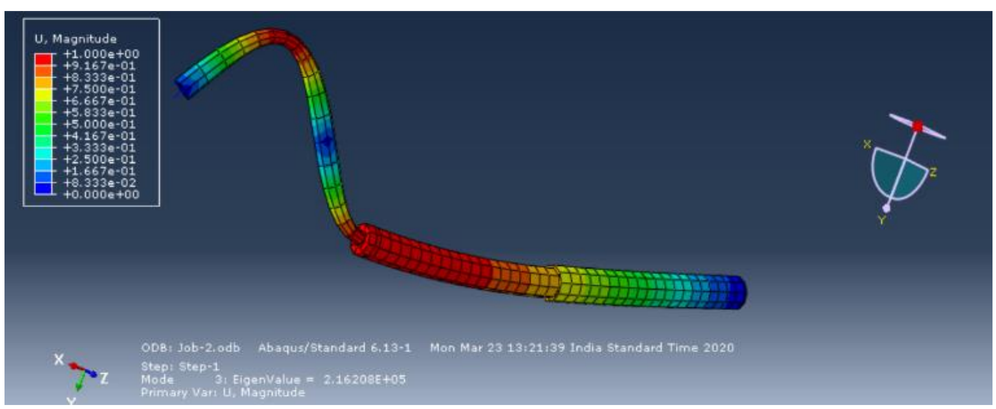


(c.)

**Figure 4.7:** (a)-(c) Eigenvalue buckling load for 515 mm, 475 mm long cylinder tube in 1st and 2nd stage respectively with piston rod of length 465 mm with mode shape 1st, 2nd and 3rd respectively considering clearance of 0.325 mm at the tip of 2nd stage cylinder tube and piston rod.

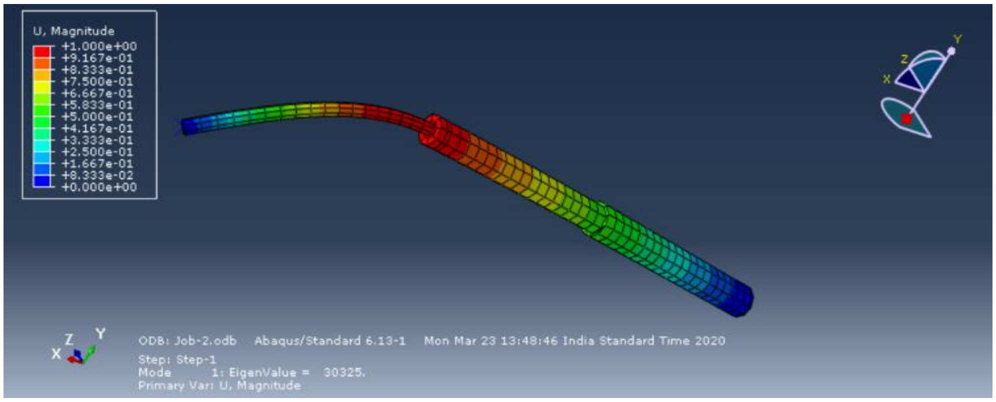


(a.)

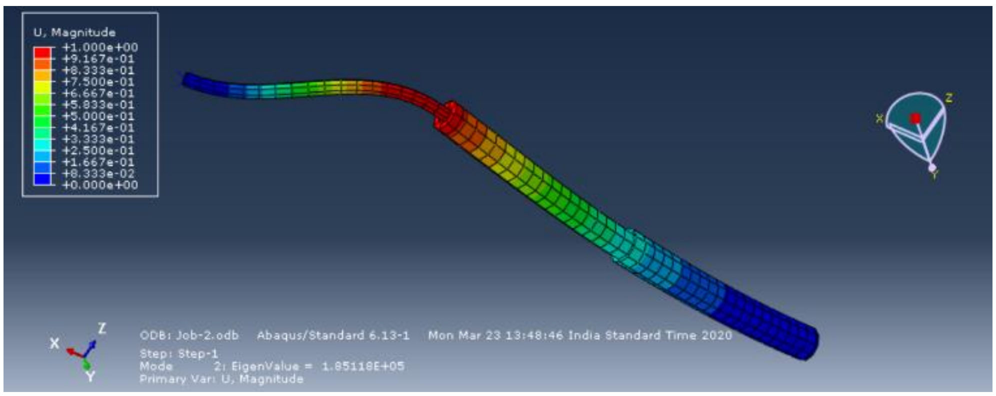


(b.)

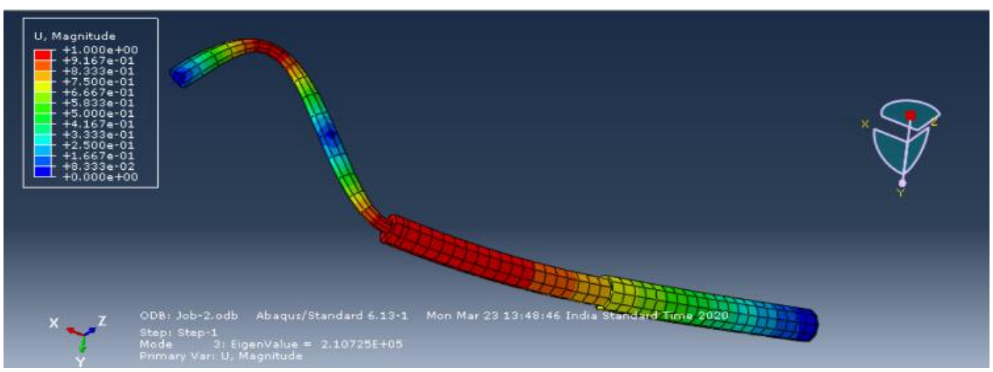


(c.)

**Figure 4.8:** (a)-(c) Eigenvalue buckling load for 515 mm, 475 mm long cylinder tube in 1$^{st}$ and 2$^{nd}$ stage respectively with piston rod of length 465 mm with mode shape 1$^{st}$, 2$^{nd}$ and 3$^{rd}$ respectively considering clearance of 0.50 mm at the tip of 2$^{nd}$ stage cylinder tube and piston rod.

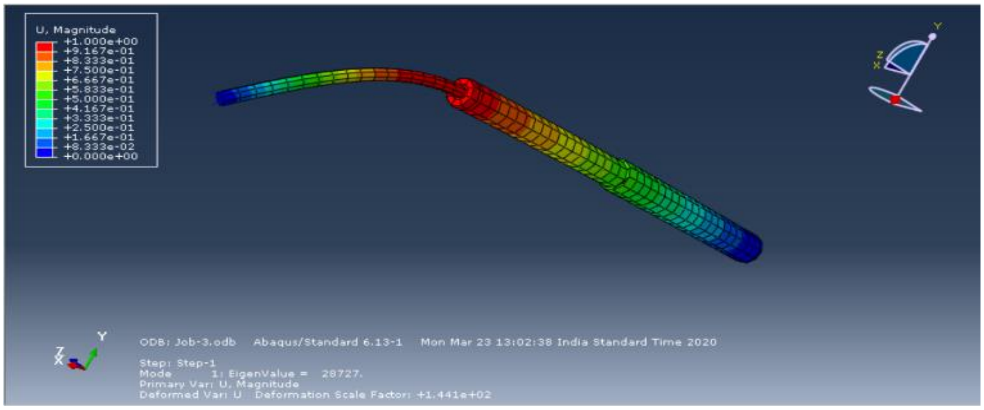


(a.)

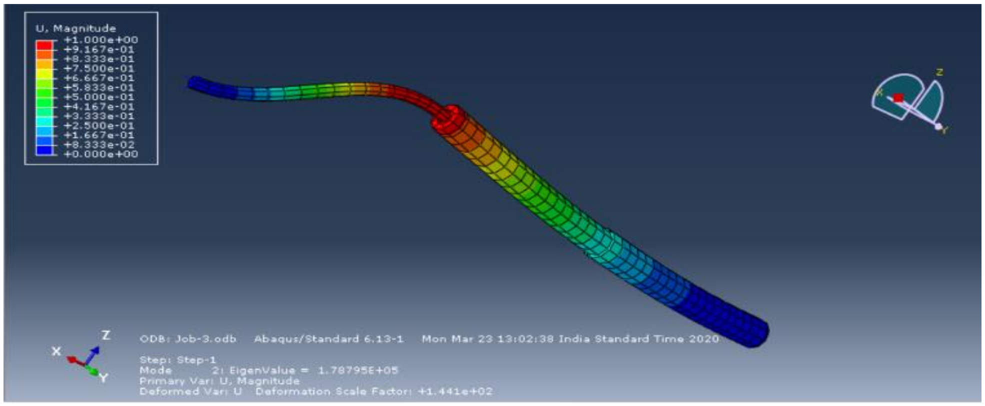


(b.)

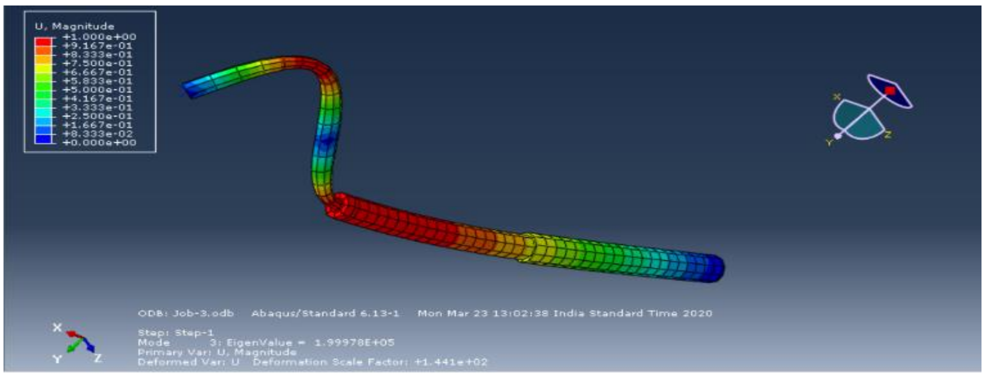


(c.)

**Figure 4.9:** (a)-(c) Eigenvalue buckling load for 515 mm, 475 mm long cylinder tube in 1st and 2nd stage respectively with piston rod of length 465 mm with mode shape 1st, 2nd and 3rd respectively considering clearance of 0.85 mm at the tip of 2nd stage cylinder tube and piston rod.

## 4.4 Results

### 4.4.1 Comparison of analytical method with FEA simulation considering no clearance

The percentage deviation between the numerical simulation and analytical method are given in Table 4.2. Buckling load vs total effective length of the cylinder tube and piston rod is shown in Figure 4.10. Buckling load increases as the effective length of the cylinder decreases and vice-versa. The graph shows that there is promisable percentage deviation between the analytical method and FEA Simulation.

**Table 4.2:** Percentage deviation between numerical simulation and analytical method.

| **Length *(l in mm)*** | **Buckling Load (N) using** | | **% Deviation** |
|---|---|---|---|
| | **Numerical simulation** | **Analytical method** | |
| **1501.5** | 28287 | 27258 | 3.6 |
| **1441.5** | 32184 | 29574.88 | 8% |
| **991.5** | 70806 | 62512.50 | 11.71% |
| **751.5** | 128816 | 108816.398 | 15.5% |

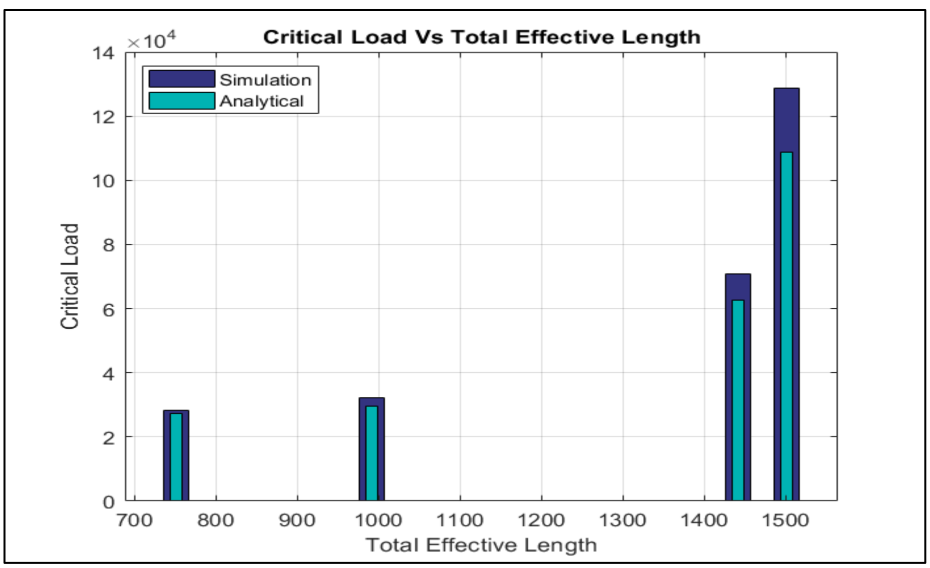


**Figure 4.10:** Buckling load vs total effective length.

### 4.4.2 Comparison of analytical method with FEA simulation considering clearance

Table 4.3 shows the results of the finite element analysis and the percentage deviation between numerical simulation and analytical method considering clearance of effective length 1441.5 mm. In Figure 4.11, a variation of analytical method and numerical simulation considering different clearance for cylinder tube 2 and piston rod with total effective length 1441.5 mm is shown. Buckling load decreases as the clearance between cylinder tube 2 and piston rod increases.

**Table 4.3:** Percentage deviation between numerical simulation and analytical method considering clearance of effective length 1441.5 mm.

| **Clearance between cylinder 2 & piston (in mm)** | 0.325 | 0.50 | 0.85 |
|---|---|---|---|
| **Buckling load using numerical simulation (N)** | 31143 | 30325 | 28727 |
| **Buckling load using an analytical method (N)** | 28080.86 | 27259.17 | 25671.14 |
| **%Deviation** | 9.80 | 10.10 | 10.60 |

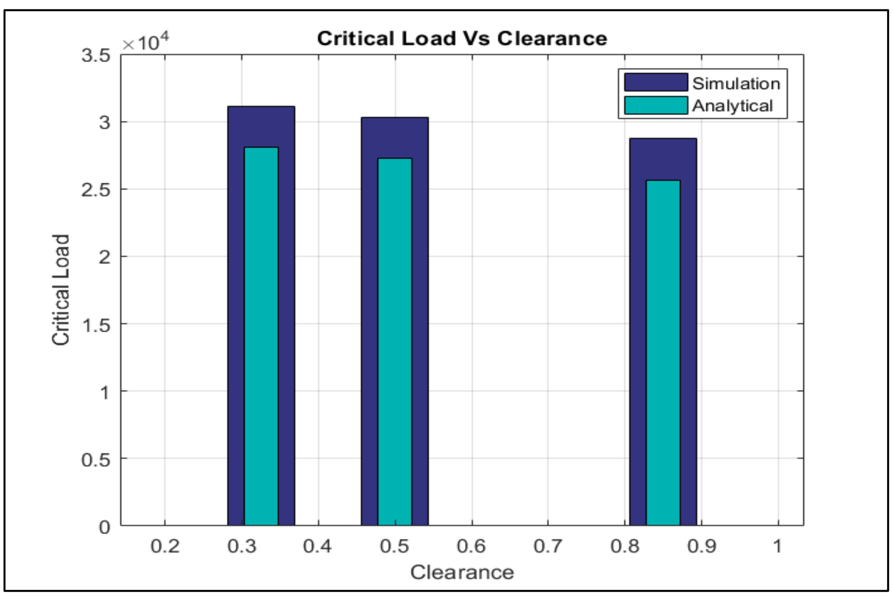


**Figure 4.11:** Variation of analytical method and numerical simulation considering clearance for cylinder tube 2 and piston rod with effective length 1441.5 mm.

# Chapter 5

# Conclusions and Future Work

## 5.1 Conclusions

In the presented research work, an innovative and convenient approach to govern the eigenvalue buckling load of the two-stage telescopic hydraulic cylinder has been presented using the analytical and finite element analysis approach. The summary of the conclusions drawn from this study are listed below:

- The theoretical approximation of the buckling load of both ends hinged hydraulic cylinder has been performed using a successive approximation method.
- The study shows a good vicinity of the buckling load has been achieved in the second iteration of this method.
- The numerical simulation has also been employed to validate the results obtained in this study.
- The outcomes of this method can be a more efficient way to evaluate the critical load-carrying capacity of a two-stage hydraulic cylinder for industrial purposes.

## 5.2 Future work

Although many aspects for the design consideration of the telescopic hydraulic cylinder have been discussed, still lots of research gaps can be listed as future scope of this research work.

i This research deals with the two-stage single acting hydraulic cylinder, multistage hydraulic cylinder analysis can be analyzed.

ii Condition monitoring of hydraulic cylinder can be performed.

iii Thermal analysis of the system can also be done.

iv Buckling load for different end condition can also be focused.

# REFERENCES

[1] Hoblit, F. (1950). Critical buckling for hydraulic actuating cylinders. Stress Engineer, Lockheed Aircraft Corporation. Product Engineering, 108-112.

[2] Seshasai, K. L., Dawkins, W. P., & Iyengar, S. (1975, October). “Stress analysis of hydraulic cylinders”. In Oklahoma State University, National Conference of fluid power.

[3] Ravishankar, N. (1981). Finite element analysis of hydraulic cylinders. Journal of Mechanical Design, 103(1), 239-243.

[4] ANSI/(NFPA) T3.6.37:1998. Method of determining the buckling load, hydraulic fluid power cylinders. NFPA Inc., uSA, 1998.

[5] Baragetti, S., & Terranova, A. (1999). “Limit load evaluation of hydraulic actuators”. International Journal of Materials and Product Technology, 14(1), 50-73.

[6] Baragetti, S., & Terranova, A. (2001). “Bending behaviour of double-acting hydraulic actuators”. Proceedings of the Institution of Mechanical Engineers, Part C: Journal of Mechanical Engineering Science, 215(5), 607-619.

[7] Hydraulic fluid power-cylinders: method for determining the buckling load, Tech. Rep. ISO/TS 13725, ISO Standard.

[8] Codina, E., & Salazar, E. (2005). Capacidad De Carga De Cilindros Oleohidráulicos: Norma ISO/TS 13725" Hydraulic fluid power-cylinders-method for determining the buckling load". Scientia et technica, 11(29), 163-168.

[9] Cai, W., Wen, Z., Jin, X., & Zhai, W. (2007). Dynamic stress analysis of rail joint with height difference defect using finite element method. Engineering Failure Analysis, 14(8), 1488-1499.

[10] Gamez-Montero, P. J., Salazar, E., Castilla, R., Freire, J., Khamashta, M., & Codina, E. (2009). “Misalignment effects on the

load capacity of a hydraulic cylinder”. International Journal of Mechanical Sciences, 51(2), 105-113.

[11] Gamez-Montero, P. J., Salazar, E., Castilla, R., Freire, J., Khamashta, M., & Codina, E. (2009). “Friction effects on the load capacity of a column and a hydraulic cylinder”. International Journal of Mechanical Sciences, 51(2), 145-151.

[12] Uzny, S. (2009). Free vibrations and stability of hydraulic cylinder fixed elastically on both ends. PAMM, 9(1), 303-304.

[13] Shariati, M., Sedighi, M., Saemi, J., & Eipakchi, H. R. (2010). An experimental study on buckling and post-buckling behaviour of cylindrical panels with clamped and simply supported ends.

[14] Sui, X. H., & Miao, D. J. (2010). Design and analysis of three-stage hydraulic cylinder used in dump trucks based on Pro/E and ANSYS. In 2010 International Conference on Mechanic Automation and Control Engineering (pp. 536-538). IEEE.

[15] Sui, X. H., Miao, D. J., & Feng, Z. M. (2010). Design and Study of Heavy Tipper Multistage Hydraulic Cylinder Based on CAD/CAE. In Advanced Materials Research (Vol. 139, pp. 1122-1125). Trans Tech Publications Ltd.

[16] Tomski, L., & Uzny, S. (2011). A hydraulic cylinder subjected to Euler's load in aspect of the stability and free vibrations taking into account discrete elastic elements. Archives of civil and mechanical engineering, 11(3), 769-785.

[17] Muppavarapu R. (2011) Nonlinear finite element analysis of columns, aerospace engineering. MS Thesis, The University of Texas, Arlington, TX, USA.

[18] Flügge, W. (2013). Viscoelasticity. Springer Science & Business Media.

[19] Wang, X., Yang, Z., Feng, J., & Liu, H. (2013). Stress analysis and stability analysis on doubly-telescopic prop of hydraulic support. Engineering Failure Analysis, 32, 274-282.

[20] DNVGL-CG-0194:2015, Class guideline - Hydraulic cylinders, Norway, 2015.

[21] Wangikar, S., Patil, A., & Patil, S. (2015). Design and buckling analysis of multistage hydraulic lifter. Design and buckling analysis of multistage hydraulic lifter, 2(8), 1953-1957.

[22] DNVGL-RP-C208:2016, Recommended Practice, Norway, 2016.

[23] Baragetti, S., & Villa, F. (2016). Effects of geometrical clearances, supports friction, and wear rings on hydraulic actuators bending behavior. Mathematical Problems in Engineering, 2016.

[24] Uzny, S., Sokół, K., & Kutrowski, Ł. (2016). Stability of a Hydraulic Telescopic Cylinder Subjected to Euler's Load. In 1st Renewable Energy Sources-Research and Business (RESRB-2016), June 22-24 2016, Wrocław, Poland (pp. 581-588). Springer, Cham.

[25] Ramasamy, V., & Basha, A. J. (2017). Multistage hydraulic cylinder buckling analysis by classical and numerical methods with different mounting conditions. In Fluid Mechanics and Fluid Power–Contemporary Research (pp. 901-910). Springer, New Delhi.

[26] Ramasamy, V., & Junaid Basha, A. M. (2018). Effect of Internal Clearance on Buckling of Multistage Hydraulic Cylinder. Defence Science Journal, 68(2).

[27] Jatin, P., Aniket, N., Kankar, P. K., Gupta, V. K., Jain, P. K., Ravindra, T., ... & Ismail, M. (2019). Estimation of Load Carrying Capacity for Pin-Mounted Hydraulic Cylinders. In Advances in Engineering Design (pp. 173-185). Springer, Singapore.

[28] Prakash, J., Gupta, S. K., & Kankar, P. K. (2020). An analytical approach to evaluate the maximum load carrying capacity for pin-mounted telescopic hydraulic cylinder. Proceedings of the Institution of Mechanical Engineers, Part C: Journal of Mechanical Engineering Science, 0954406220916524.

[29] Timoshenko, S. (1970). Theory of Elastic Stability 2e. Tata McGraw-Hill Education.

[30] Dbcompressor (2016), www.dbcompressor.com OR: CEC (2016), http://dbcompressor.com/wp-content/uploads/2016/10/Hydraulic_Cylinder_Cutaway.png